Electric and plasma characteristics of RF discharge plasma actuation under varying pressures*

Huimin Song(宋慧敏)†, Min Jia(贾敏), Di Jin(金迪), Wei Cui(崔巍), and Yun Wu(吴云)

Science and Technology on Plasma Dynamics Laboratory, Air Force Engineering University, Xi'an 710038, *China*

(Received 14 May 2015; revised manuscript received 12 November 2015; published online 20 January 2016)

The electric and plasma characteristics of RF discharge plasma actuation under varying pressure have been investigated experimentally. As the pressure increases, the shapes of charge–voltage Lissajous curves vary, and the discharge energy increases. The emission spectra show significant difference as the pressure varies. When the pressure is 1000 Pa, the electron temperature is estimated to be 4.139 eV, the electron density and the vibrational temperature of plasma are 4.71×10^{11} cm^{-3} and 1.27 eV, respectively. The ratio of spectral lines $I^{\rm peak}_{391.4}/I^{\rm peak}_{380.5}$ which describes the electron temperature hardly changes when the pressure varies between 5000–30000 Pa, while it increases remarkably with the pressure below 5000 Pa, indicating a transition from filamentary discharge to glow discharge. The characteristics of emission spectrum are obviously influenced by the loading power. With more loading power, both of the illumination and emission spectrum intensity increase at 10000 Pa. The pin–pin electrode RF discharge is arc-like at power higher than 33 W, which results in a macroscopic air temperature increase.

Keywords: plasma aerodynamic actuation, optical emission spectrum, plasma flow control, RF discharge

PACS: 52.50.Nr, 52.80.Mg, 47.80.Jk **DOI:** 10.1088/1674-1056/25/3/035204

1. Introduction

Plasma flow control based on plasma aerodynamic actuation, is an active flow control technique. It is very promising on lift enhancement and drag reduction of aircraft and stability expansion of aero-engine.[1–7]

The plasma aerodynamic actuation generated by dielectric barrier discharge (DBD) has been intensively investigated by researchers all over the world. Compared with DBD, RF discharge has advantages, such as stable volume discharge in high-speed airflow, and simple power tuning, which has drawn increasing attention for its potential application on both low and high speed flow control.[8–13]

Leonov *et al.* experimentally and theoretically investigated the dynamics of a single-electrode RF filament in supersonic airflow by means of optical emission spectrum and Schlieren visualization. It is revealed that the gas temperature in filamentary RF plasma can reach up to 4000 K at a static pressure of 120 Torr. RF discharge plasma filaments were proved effective on shock position and intensity control.[8] Klimov *et al.* experimentally investigated the surface RF plasma aerodynamic actuator in subsonic and supersonic airflow. Experimental results showed that surface RF discharge consists of many plasma filaments, which increase the surface pressure and decrease the stagnation pressure.[9,10] Bityurin *et al.* presented experimental and numerical results of the surface RF discharge at a conical body in airflow. Significant flow modification has been achieved between Mach number 0.5–2.0.[11] RF discharge was also adopted in their experiments for flow control around wing model and jet noise control.[8–13] Dedrick investigated the electrical and optical characteristics of RF asymmetric surface barrier discharge plasma in atmospheric pressure air.[14,15]

For practical purpose, the working altitude of plasma flow control is designed from 0 km to as high as 30 km, within which the static pressure changes influence RF discharge significantly. In this paper, the electric and plasma characteristics of RF discharge plasma actuation under varying pressure are investigated experimentally.

2. Experimental setup

The schematic diagram of experimental setup is shown in Fig. 1. The experiment is conducted in a pressure chamber. The operating pressure is varied between 200 Pa and 1×10^5 Pa. The gas temperature is assumed to be 300 K.

2.1. Plasma actuation system

An RF generator/amplifier (AG 1017L, T&C) is adopted, which is a totally solid-state, air-cooled RF power source expressly designed for use in general ultrasonic and gas plasma applications. The maximum power output of AG 1017L is 500 W and the operating frequency varies from 10 kHz to 10 MHz. A pin–pin plasma actuator includes a pair of pin tungsten electrodes and a bakelite holding device. The pin–pin electrodes are aligned with a 0.5-mm gap between tips.[16] The pin–to–pin plasma actuator is fixed in the pressure chamber, located 5 cm away from the quartz observing window. An impedance matching circuit, which consists of inductors and capacitors, is designed to confirm impedance matching of RF generator and plasma actuator.

*Project supported by the National Natural Science Foundation of China (Grant Nos. 11472306, 51336011, and 51407197).

†Corresponding author. E-mail: min_cargi@sina.com

© 2016 Chinese Physical Society and IOP Publishing Ltd

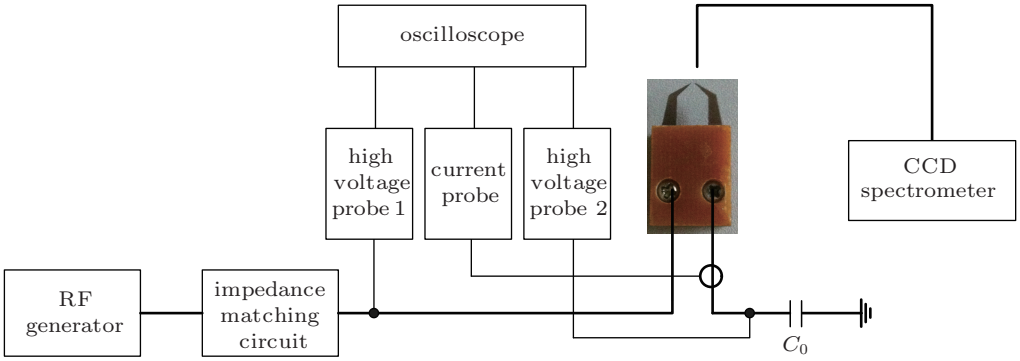


Fig. 1. (color online) Schematic diagram of experiment setup.

2.2. Diagnostic system

The voltage applied on the plasma actuator is measured with a high voltage probe 1 (P6015A, Tektronix), while the discharge current is measured with a current probe (TCP0030A, Tektronix). The capacitance C_0 was connected in the circuit, so as to calculate the conduction charge. The voltage between the capacitance is measured by high voltage probe 2. These signals are displayed and recorded through an oscilloscope (DPO4104, Tektronix). The optical emission spectra are obtained with a charge coupled device spectrometer (Avantes USB2048) and the emission intensity is averaged temporally and spatially.

3. Experimental results

3.1. Electric characteristics

In order to acquire the influence of pressure, the images, voltages, and currents of RF discharge under different pressures are recorded and the effect of pressure on the charge–voltage Lissajous curves is also experimentally investigated.

3.1.1. Morphology of RF discharge

The images of RF discharge under different pressures are shown in Fig. 2. The frequency of RF generator is set to be 1.45 MHz, which is the impedance matching frequency of RF generator and plasma actuator. P_{I} represents the output power of RF power supply, while P_{L} is defined as the power being loaded onto the plasma actuator.

When the pressure is 500 Pa, the loading power (P_{L}) is 12 W, and dim bluish violet light can be observed on the plasma actuator. With the increase of pressure and loading power, the luminous intensity increases. When the pressure is 96000 Pa, there is bright white light between the electrode tips. Figure 2 shows that it is easier to acquire and maintain glow discharge under lower pressure. Instead of being restricted between pin–pin electrode tips, the discharge spreads all over the electrodes and radiates outward (as shown in Figs. 2(a)–2(c)). Under atmosphere, if the breakdown happens without decreasing the power of RF generator, the glow discharge will change into the arc mode and erodes the electrodes (as shown in Fig. 2(d)). It can be explained as follows: as the pressure increases, the electron energy relaxation length decreases and high-energy electrons produced in the strong electric field between tips cannot diffuse to the whole electrodes, so the discharge is confined in the gap between two tips.

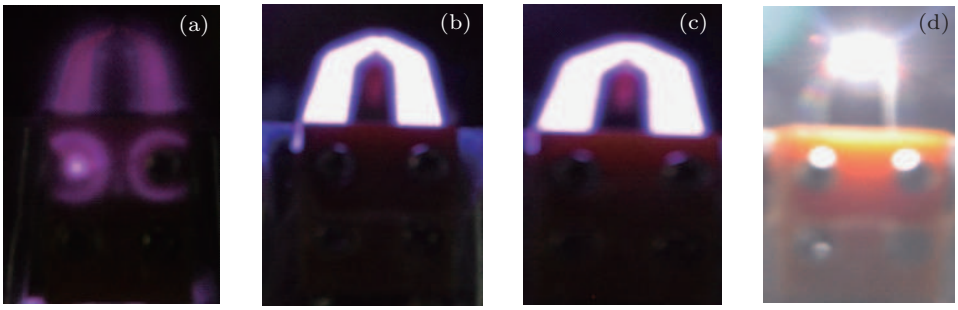


Fig. 2. (color online) Images of RF discharge under different pressures. (a) 500 Pa, $P_{\mathrm{L}} = 12$ W, (b) 20000 Pa, $P_{\mathrm{L}} = 19$ W, (c) 60000 Pa, $P_{\mathrm{L}} = 47$ W, (d) 96000 Pa, $P_{\mathrm{L}} = 100$ W.

3.1.2. Discharge voltage and current

The voltage–current plots of RF discharge under different pressures are shown in Fig. 3. The voltage plots are smooth and continuous, which has the same frequency of the carrier wave from RF generator (1.45 MHz). Since the load of pin–pin electrodes actuator is capacitive, there is a phase difference

between voltage and current under each pressure. When the pressure is below 60000 Pa, the positive half period and negative one are symmetric, and the intensity and number of current pulse are basically the same. However, the positive and negative half period of the current curves become asymmetric when the pressure and power are relatively higher. It can be explained as follows: under low pressure, the density of molecules is lower, it is difficult for molecules to capture electrons and form negative space charges, so there is little difference observed between the positive and negative half period. While with the increase of pressure, the space charge accumulation results in an electric field distortion, which makes the distribution of electric field more different between the positive and negative half period, and the discharge characteristic also shows distinction. Additionally, with the increase of discharge energy, the influence of space charge becomes stronger, and the difference of discharge between the positive and negative half period is even bigger.

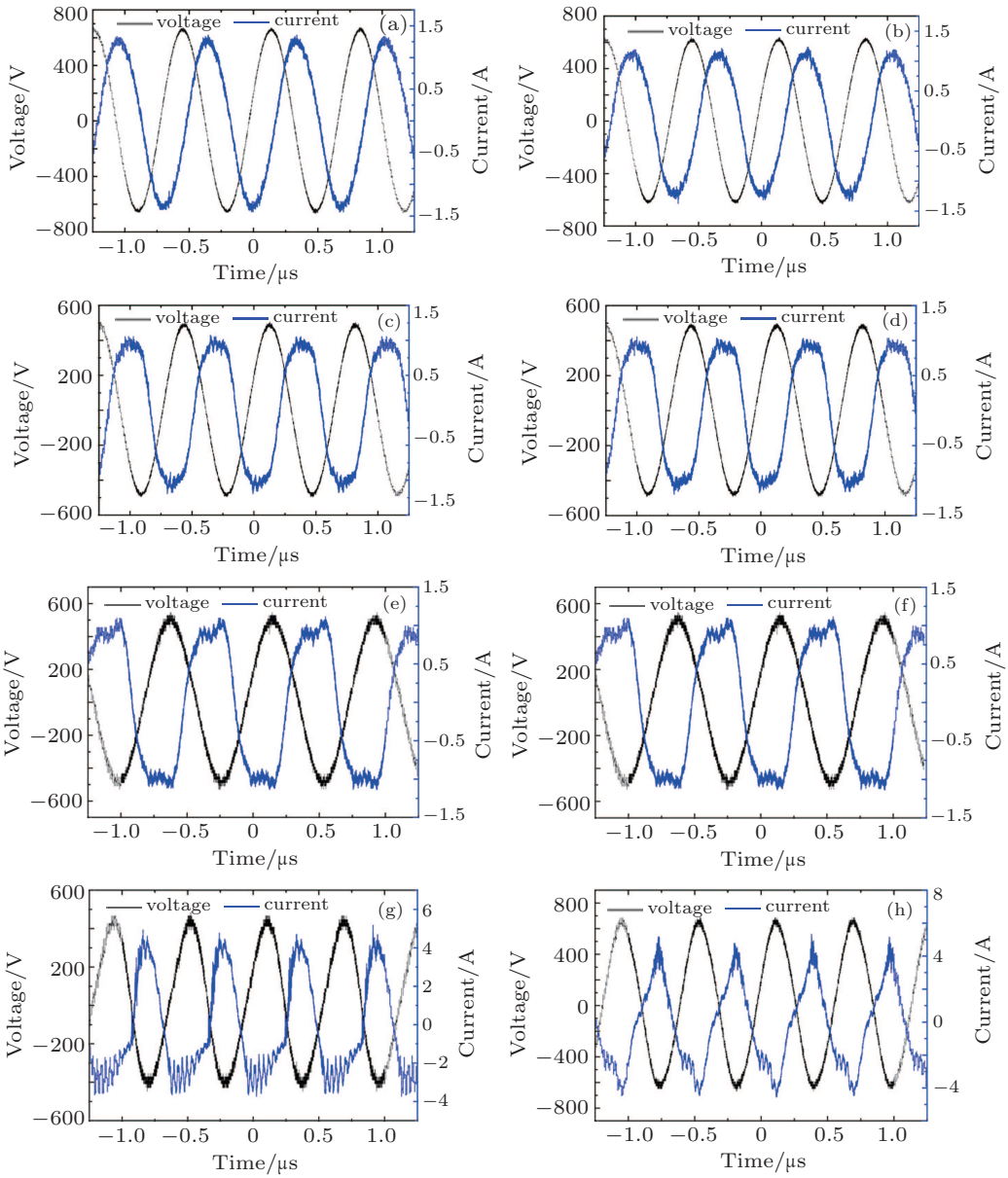


Fig. 3. (color online) The V–I plots of RF discharge under different pressures. (a) 500 Pa, $P_{\rm L} = 12$ W; (b) 1000 Pa, $P_{\rm L} = 15$ W; (c) 5000 Pa, $P_{\rm L} = 18$ W; (d) 20000 Pa, $P_{\rm L} = 19$ W; (e) 40000 Pa, $P_{\rm L} = 25$ W; (f) 60000 Pa, $P_{\rm L} = 47$ W; (g) 70000 Pa, $P_{\rm L} = 85$ W; (h) 96000 Pa, $P_{\rm L} = 100$ W.

3.1.3. Lissajous curves of RF discharge

With charge–voltage Lissajous figures, discharge parameters such as electrode gap, dielectric equivalent capacitance, voltage between electrode gap, peak voltage, discharge power, discharge energy, and so on, can be calculated.[17] The Lissajous figures of pin–pin electrodes RF discharge under different pressures are shown in Fig. 4. Under various pressures, all the Lissajous curves are closed. With the increase of pressure,

the shapes of Lissajous curves change, and the scatters of Lissajous curves become more concentrated as discharge power increases.

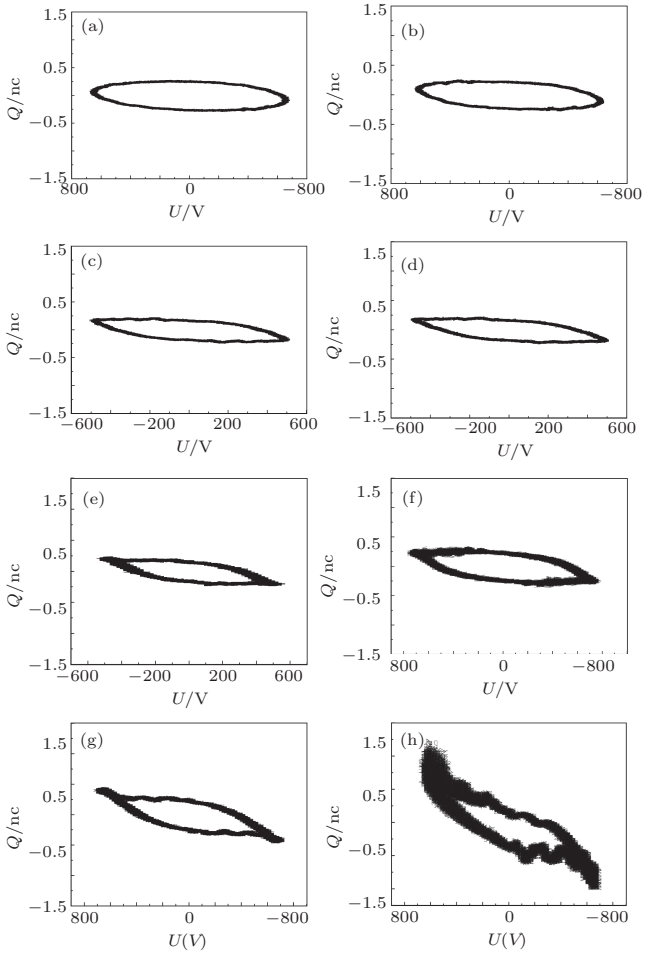


Fig. 4. (color online) The Lissajous figures of RF discharge under different pressures. (a) 500 Pa, $P_{\rm I} = 20$ W, $P_{\rm L} = 12$ W; (b) 1000 Pa, $P_{\rm I} = 20$ W, $P_{\rm L} = 15$ W; (c) 5000 Pa, $P_{\rm I} = 20$ W, $P_{\rm L} = 18$ W; (d) 20000 Pa, $P_{\rm I} = 20$ W, $P_{\rm L} = 19$ W; (e) 40000 Pa, $P_{\rm I} = 50$ W, $P_{\rm L} = 25$ W; (f) 60000 Pa, $P_{\rm I} = 70$ W, $P_{\rm L} = 65$ W; (g) 70000 Pa, $P_{\rm I} = 92$ W, $P_{\rm L} = 76$ W; (h) 96000 Pa, $P_{\rm I} = 140$ W, $P_{\rm L} = 100$ W.

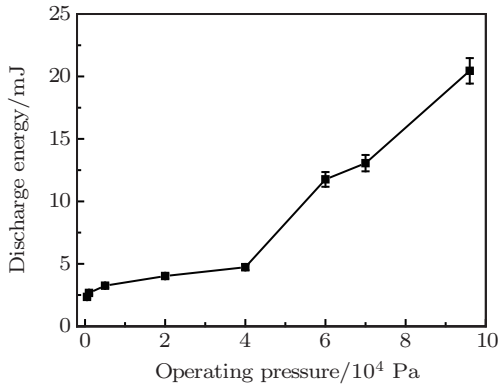


Fig. 5. Discharge energy under different pressures.

The relationship between Lissajous figures and discharge energy is linear. The discharge energy of one period ($E(L)$) can be written as

$$E(L) = \int Q\mathrm{d}V = A_{\rm Lissajous}. \tag{1}$$

Here, V is the applied voltage, and Q is the electric charge being transported during the discharge.

The discharge energy under varying pressures, which is calculated from the Lissajous curves in Fig. 4, is shown in Fig. 5. Below 40000 Pa, the discharge energy slightly increases with increasing pressure, while it increases remarkably with pressure increasing between 40000 Pa and 96000 Pa.

3.2. Emission characteristics

As an effective non-intrusive diagnostic method, optical emission spectroscopy is widely used to investigate air plasma.[18–21] In this paper, optical emission spectroscopy of RF discharge plasma was measured under varying operating pressures and loading powers.

3.2.1. Optical emission spectrum at 1000 Pa

The emission spectral characteristics of RF discharge have been firstly investigated under low pressure. The emission spectrum of pin–pin electrodes RF discharge is shown in Fig. 6. The actuator is placed in the vacuum chamber with pressure of 1000 Pa, the peak–peak voltage and pulse frequency are 1.3 kV and 1.45 MHz, respectively. The integration time of spectrometer is set to be 2000 ms. Outside the quartz glass window, the head of optical fiber is 5 cm away from the gap between electrodes and aimed at it. The spectral line between 300–450 nm shows similarity with the line of low pressure DBD.[24]

The emission spectrum between 300 nm and 450 nm is analyzed, as shown in Fig. 7. The luminescent particles are mainly $N_2(C^3\Pi_u)$ molecules and $N_2^+(B^2\Sigma_u^+)$ ions.

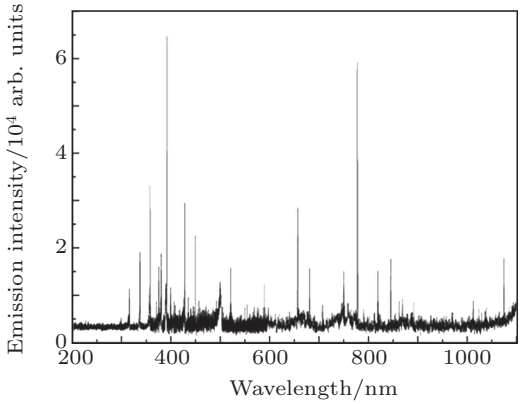


Fig. 6. Emission spectrum of pin–pin electrode RF discharge at 1000 Pa.

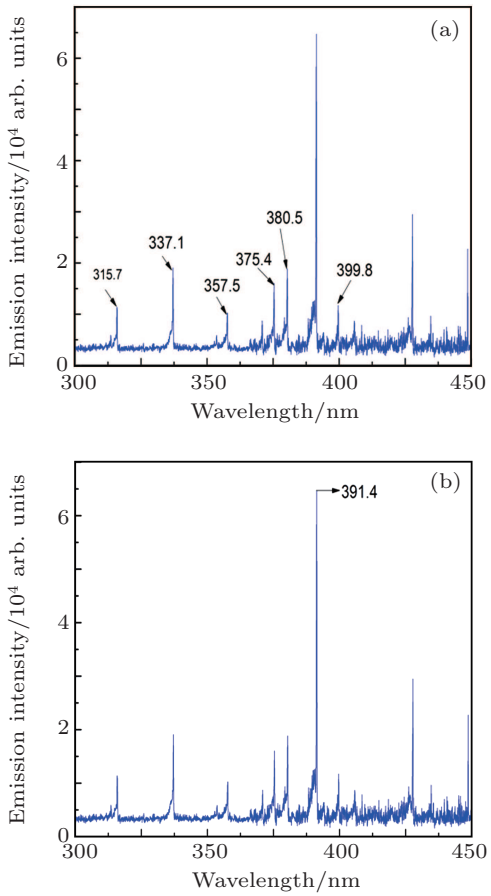


Fig. 7. (color online) Emission spectrum of (a) $N_2(C^3\Pi_u)$ and (b) $N_2^+(B^2\Sigma_u^+)$.

3.2.1.1. Electron temperature

Suppose that the electrons follow Maxwell distribution, the electron temperature can be adopted to feature the energy distribution of electrons (about two thirds of the average kinetic energy of electron).[22–24] Similarly, for Maxwell distribution, the equivalent electron temperature can also be defined with average energy. In plasma, the excited molecules, ions, and active particles are created by the collision of electrons at different energy levels, such as the increase of average molecular velocity, the vibrational and rotational excitation of molecule, the dissociation and ionization of molecule. Therefore, the emission spectrum generated during the return of molecules from excited state to the ground state must be closely related to electron temperature.

Because the rotational energy levels are closely spaced and allow for rapid energy transfer between the two energy modes, the gas temperature is estimated by the rotational temperature of a molecular. Through fitting the N_2 second positive system band from 378 nm to 381 nm, the rotational temperature of N_2 can be obtained.[24] Under a given rotational temperature (500 K), with the dipole radiation probability and response function of the monochrometer, the profile of a certain emission band is acquired. The actual rotational temperature (T_r) is determined through comparing the experimental measurement and theoretical calculation.[24] When the operating pressure is 1000 Pa, the rotational temperature is calculated to be 500 K.

As the gas temperature changes from 300–1000 K, and the electron temperature alters from 1 eV to 4 eV, through solving the equation and acquiring the stationary solution ($dn/dt = 0$), the relationship between electron temperature and intensity rate of two spectral lines can be fitted and written as an empirical equation,

$$r_{I1} = \frac{I_{391.4}^{peak}}{I_{380.5}^{peak}}, \tag{2}$$

$$\gamma_{I1} = K_0(T_e)^{C_0} \exp\left(-\frac{E_0}{T_e}\right). \tag{3}$$

Here, the vibrational temperature of N_2 molecules (C state) caused by the change of electron density is ignored. This is reasonable because the vibrational distribution of C state N_2 molecules is similar to that of ground state N_2 molecules according to the Frank–Condon principle.

When it comes to the spectrum in Fig. 6, $r_{I1} = 3.435$ and $T_e = 4.139$ eV.

3.2.1.2. Electron density

Electron density (plasma density) is one of the important physical parameters which describes the characteristics of discharge plasma. To some degree, it could represent the ions which participate in the momentum transfer.[22–24]

According to the balance equation of $N_2(C)$ and $N_2^+(B)$,

$$\frac{dn_C}{dt} = n_e n_{N_2} Q_C - A_C n_C - n_C n_{N_2} Q_{N_2} - n_C n_{O_2} Q_{O_2}, \tag{4}$$

$$\frac{dn_{B+}}{dt} = n_e n_{N_2} Q_{B+} - A_{B+} n_{B+} - n_{B+} n_{N_2} Q_{N_2} - n_{B+} n_{O_2} Q_{O_2}. \tag{5}$$

The relative density of ground state N_2 at different vibrational level is mainly depending on the electron density. Based on Frank–Condon principle, the distribution change of ground-state vibrational level can be reflected by the distribution of C state vibrational level.

As the temperature varies from 300 K to 1000 K, and the electron ionization rate temperature alters from 10^{-10} to 10^{-5}, through solving the equation and acquiring the stationary solution ($dn/dt = 0$), the relationship between electron density and intensity rate of two spectral lines can be fitted and written as an empirical equation,

$$r_{I2} = \frac{I_{371.1}^{peak}}{I_{380.5}^{peak}}, \tag{6}$$

$$r_{I2} = C_0 + C_1 \log_{10}(n) + C_2 (\log_{10} n)^2. \tag{7}$$

Here, the influence of pressure, electron temperature, and air temperature is so small that can be ignored. This is because these two lines are emitted by excited states mainly produced by electron-impact excitation of the same ground state N_2

molecules. Since the electron excitation energy is very close, this line ratio is insensitive to the electron temperature.

For the spectrum shown in Fig. 6, $r_{I2} = 0.464$ and $n_e = 4.7 \times 10^{11}$ cm^{-3}.

3.2.1.3. Vibrational temperature

The intensity of molecule vibrational excitation is represented as vibrational temperature T_v, which is one of the important parameters of plasma[22–24]

$$r_{I2} = \frac{I^{peak}_{371.1}}{I^{peak}_{380.5}}, \tag{8}$$

$$r_{I2} = 1.1384 \exp(-0.4952/T_v). \tag{9}$$

For the spectrum shown in Fig. 6, $r_{I2} = 0.464$ and $T_v = 1.27$ eV.

It is believed that vibrational excitation is one of the important aspects of electron energy loss. For one thing, the collision cross section is big; for another, the electron is at lower energy state, and the excitation state is weaker.

3.2.2. Influence of operating pressure on optical emission characteristics

With the RF generator output power of 20 W, the influence of operating pressure (1000–30000 Pa) on RF discharge plasma is investigated. Optical emission spectrum under various pressures is shown in Fig. 8. When the operating pressure is above 30000 Pa, RF discharge cannot be formed under given conditions.

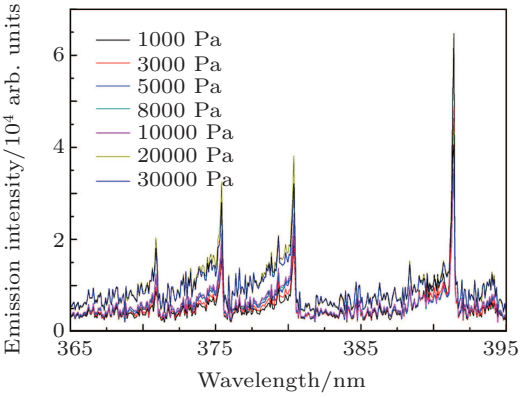


Fig. 8. (color online) Optical emission spectrogram under varying pressures (365–395 nm).

Relative intensity ratio from 391.4 nm to 380.5 nm ($I^{peak}_{391.4}/I^{peak}_{380.5}$), which indicates electron temperature, versus the operating pressure is shown in Fig. 9. The $I^{peak}_{391.4}/I^{peak}_{380.5}$ remains almost unchanged when the operating pressure is from 5000 Pa to 30000 Pa. When the operating pressure is below 5000 Pa, the intensity ratio $I^{peak}_{391.4}/I^{peak}_{380.5}$ increases with the decrease of operating pressure, which indicates the discharge mode change from filamentary discharge to glow discharge at around 5000 Pa. It is in accordance with Choi's conclusion on the volumetric dielectric barrier discharge mode in the air.[18]

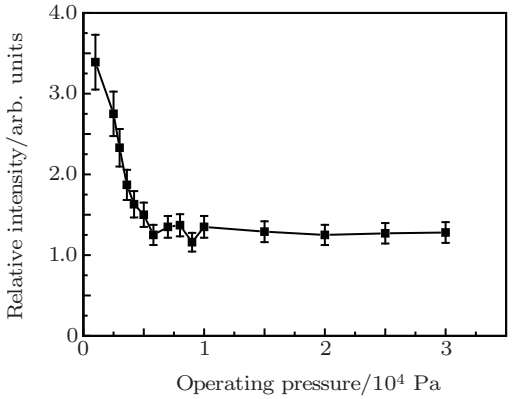


Fig. 9. Relative intensity ratio from 391.4 nm to 380.5 nm ($I^{peak}_{391.4}/I^{peak}_{380.5}$) under varying pressures.

Relative intensity ratio of 371.1 nm to 380.5 nm ($I^{peak}_{391.4}/I^{peak}_{380.5}$), which indicates electron density and vibrational temperature, versus operating pressure is shown in Fig. 10. It remains almost unchanged with the decreasing operating pressure.

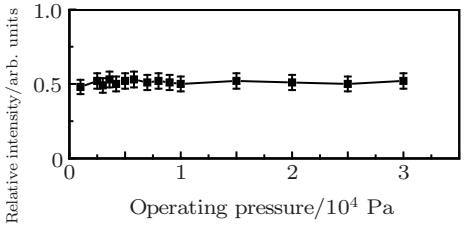


Fig. 10. Relative intensity ratio from 371.1 nm to 380.5 nm ($I^{peak}_{391.4}/I^{peak}_{380.5}$) under varying pressures.

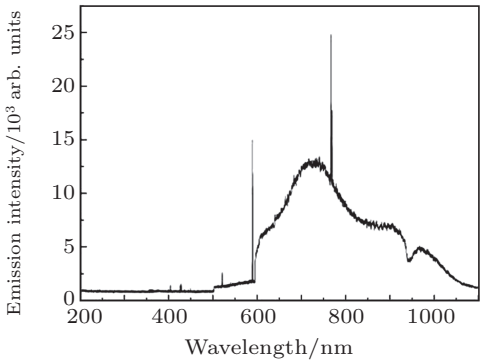


Fig. 11. Optical emission spectrogram with the operating pressure of 96000 Pa.

When the operating pressure is 96000 Pa and P_L is 100 W, the optical emission spectrogram of RF discharge is shown in Fig. 11, which is obviously different from that with lower operating pressure and power input (see Figs. 6 and 8). As the intensity of RF discharge increases apparently, the exposure time of spectrometer is adjusted to be 50 ms. As the exposure time becomes much shorter, the optical emission spectrum of 300–450 nm is very weak. While the spectrum of 600–1100 nm increases remarkably, showing that the gas temperature is much higher than that under lower operating pressures.

3.2.3. Influence of loaded power on optical emission characteristics

The influence of loaded power on RF discharge plasma was investigated when the operating pressure is fixed at 10000 Pa. Figure 12 shows the optical emission spectrogram of RF discharge plasma with various loaded powers. When $P_{\rm I}$ was 20 W and $P_{\rm L}$ was 14 W, the optical emission spectrogram was shown in Fig. 12(a). The intensity of emission spectrogram shown in Fig. 12(b) is acquired with $P_{\rm I}$ of 30 W and $P_{\rm L}$ of 23 W. The exposure time is set to be 1000 ms in both experiments. The intensity of emission spectrum between 600–1100 nm increases at $P_{\rm L}$ of 23 W. The optical emission spectrogram with $P_{\rm L}$ of 33 W and $P_{\rm I}$ of 40 W is shown in Fig. 12(c). As the intensity of emission spectra becomes even higher, the exposure time of spectrometer is shortened to be 500 ms, and optical emission spectra of 600–1100 nm increased remarkably.

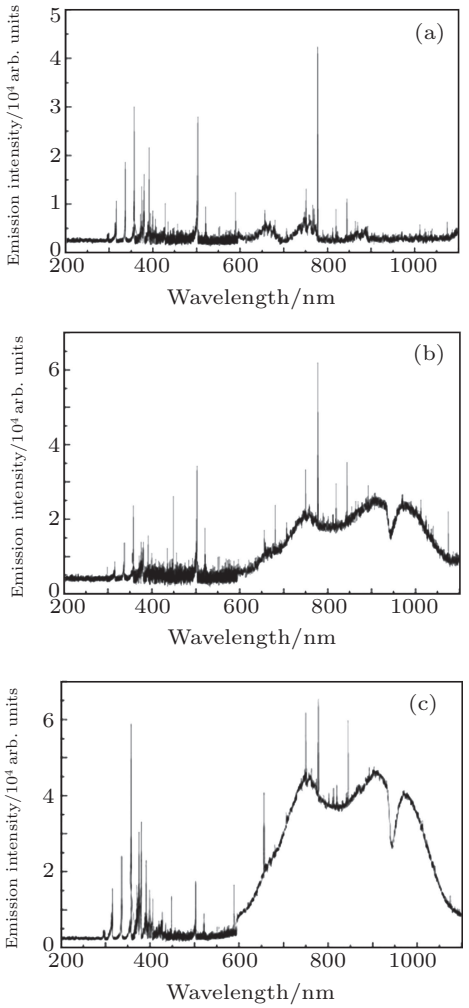


Fig. 12. Optical emission spectrogram with the operating pressure of 10000 Pa. (a) $P_{\rm L} = 14$ W, exposure time is 1000 ms; (b) $P_{\rm L} = 23$ W, exposure time is 1000 ms; (c) $P_{\rm L} = 33$ W, exposure time is 500 ms.

According to Planck's law, the spectral radiant exitance of blackbody can be written as

$$M_{\lambda \rm bb} = \frac{2\pi hc^2}{\lambda^5} \frac{1}{{\rm e}^{hc/(\lambda K_{\rm B} T)} - 1} = \frac{c_1}{\lambda_5} \frac{1}{{\rm e}^{c_2/(\lambda T)} - 1}. \quad (10)$$

Here, $M_{\lambda \rm bb}$ is the spectral radiant exitance of blackbody ($\rm W/(m^2 \cdot \mu m)$), λ is the wavelength (μm), T is the absolute temperature (K), c is the speed of light (m/s), c_1 is the first radiation constant, c_2 is the second radiation constant, and $K_{\rm B}$ is Boltzmann constant (J/K).

It can be deduced from Eq. (10) that with the increase of temperature, the spectral radiation curve is elevated, and the spectral radiant exitance is relatively bigger at any designated wavelength. The spectral radiant exitance of every wavelength is bigger, while the peak wavelength decreases, which means that the proportion of short wave component increases.[25]

The discharge temperature between pin–pin electrodes is not uniform, but obeys certain temperature distribution, so the emission spectrum is not a standard Planck line. However, the increase of optical emission intensity still indicates a rise of both maximum temperature and average temperature. Furthermore, the optical emission spectrogram of RF discharge at higher loaded power is more similar to that of carbon arc (see Figs. 4–26 in Ref. [25]). It can be concluded that as loaded power increases, the discharge is more similar to arc discharge, and the gas temperature increases obviously.

4. Conclusion and future works

The electric and plasma characteristics of RF discharge plasma actuation under varying pressure were investigated experimentally.

(i) Since the load of pin–pin electrodes is capacitive, there is a phase difference between voltage and current plots of RF discharge. Under various pressures, all the Lissajous curves are closed. With the increase of pressure, the shapes of Lissajous curves vary, and discharge energy calculated from Lissajous curve becomes larger. Below 40000 Pa, the discharge energy slightly increases with increasing pressure, while it increases remarkably with increasing pressure between 40000 Pa and 96000 Pa.

(ii) The emission spectral characteristics of RF discharge have been researched under low pressure. Based on the chemical kinetics model of air discharge luminescent particles, with the intensity ratio of spectral lines $I^{\rm peak}_{391.4}/I^{\rm peak}_{380.5}$ at 1000 Pa, the electron temperature of pin–pin electrode RF discharge is calculated to be 4.139 eV. With the intensity ratio of spectral lines $I^{\rm peak}_{371.1}/I^{\rm peak}_{380.5}$ at 1000 Pa, the electron density is calculated to be 4.71×10^{11} $\rm cm^{-3}$, and the vibrational temperature is 1.27 eV.

(iii) With the fixed power loaded on plasma actuator, relative intensity ratio from 391.4 nm to 380.5 nm ($I^{\rm peak}_{391.4}/I^{\rm peak}_{380.5}$) remains almost unchanged when the operating pressure is between 5000 Pa and 30000 Pa. When the operating pressure is below 5000 Pa, the intensity ratio $I^{\rm peak}_{391.4}/I^{\rm peak}_{380.5}$ increases with the decrease of operating pressure, which indicates that the discharge mode changes from filamentary discharge to glow discharge at around 5000 Pa. Relative emission intensity ratio from 371.1 nm to 380.5 nm ($I^{\rm peak}_{371.1}/I^{\rm peak}_{380.5}$), which repre-

sents electron density and vibrational temperature, changes little while the pressure varies between 300–30000 Pa.

(iv) When the operating pressure is 10000 Pa, the optical emission spectra with different power loaded on the actuator shows difference. The intensity of emission spectra increase with the increase of loading power. When it reaches as high as 33 W, the discharge mode of pin–pin RF discharge is arc-like, which leads to the increase of macro gas temperature.

Future work should focus on the interaction between RF discharge plasma actuation and high speed flow. Small-scaled supersonic wind tunnel test should be conducted to verify the effectiveness of RF discharge plasma actuation on shock wave control.

References

[1] Roth J R 2003 *Phys. Plasmas* **10** 2117

[2] Patel M P, Ng T T, Vasudevan S, *et al*. 2006 *AIAA* 2006–3495

[3] Li Y H, Wu Y, Zhou M, *et al*. 2010 *Exp. Fluids* **48** 1015

[4] Li Y H, Wu Y, Zhang P, *et al*. 2008 *Acta Aerodynamica Sin.* **26** 1429

[5] Moreau E 2007 *J. Phys. D: Appl. Phys.* **40** 605

[6] Corke T C, Post M L and Orlov D M 2007 *Prog. Aerosp. Sci.* **43** 193

[7] Li Y H, Wu Y, Liang H, *et al*. 2010 *Chin. Sci. Bull.* (Chin. Ver.) **55** 3060

[8] Leonov S, Bityurin V and Kolesnichenko Y 2001 39*th AIAA Aerospace Sciences Meeting & Exhibit*, January 8–11, 2001 Reno, USA

[9] Klimov A, Bitiurin V, Moralev I, Tolkunov B, Zhirnov K and Kutlaliev V 2008 46*th AIAA Aerospace Sciences Meeting and Exhibit*, January 7–10, 2008, Reno, USA

[10] Klimov A, Moralev I, Bityurin V A, Kazansky P N, Chertov D A and Borisov I A 2011 49*th AIAA Aerospace Sciences Meeting including the New Horizons Forum and Aerospace Exposition*, January 4–7, Orlando, USA

[11] Bityurin V, Bocharov A, Klimov A, *et al*. 2009 *AIAA* 2009–4073

[12] Kazansky P, Moralev I, Klimov A and Bityurin V 2012 50*th AIAA Aerospace Sciences Meeting including the New Horizons Forum and Aerospace Exposition*, January 09–12, 2012, Nashville, USA

[13] Kopiev V, Ostrikov N, Zaitsev M, Kopiev V, Belyaev I, Bityurin V, Klimov A, Moralev I and Godin S 2011 49*th AIAA Aerospace Sciences Meeting including the New Horizons Forum and Aerospace Exposition*, January 4–7, 2011, Orlando, USA

[14] Dedrick J, Boswell R W, Audiers P, *et al*. 2011 *J. Phys. D: Appl. Phys.* 205202

[15] Dedrick J, Im S, Cappelli M, *et al*. 2013 *IEEE Transactions on Plasma Science* **41** 3275

[16] Song H M, Wu W W, Cui W, Jia M, Jin D and Liang H 2014 *High Voltage Engineering* **40** 2044

[17] Jiang H, Shao T, Zhang C, Li W, Yan P and Che X K 2013 *IEEE Transactions on Dielectrics and Electrical Insulation* **20** 1101

[18] Choi J H, Lee T I, Han I, *et al*. 2006 *Plasma Sources Sci. Technol.* **15** 416

[19] Kozlov K V and Wagner H E 2007 *Contribution to Plsma Physics* **47** 26

[20] Enloe C L, McLaughlin T E, VanDyken R D, *et al*. 2004 *AIAA J.* **42** 589

[21] Borghi C A, Carraro M, Cristofolini A, *et al*. 2006 37*th AIAA Plasmadynamics and Lasers Conference*, June 5–8, 2006, San Francisco, USA

[22] Zhu X M and Pu Y K 2005 *Phys. Plasmas* **12** 103501

[23] Zhu X M and Pu Y K 2006 *Phys. Plasmas* **13** 063507

[24] Wu Y, Li Y H, Jia M, *et al*. 2010 *Chin. J. Aeronaut.* **23** 39

[25] Zhang J Q and Fang X P 2007 *Infrared Physics* (Xi'an: Xi'an Electronic Science & Technology University Press)